

# Field Tracer Tests to Evaluate Transport Properties of Tryptophan and Humic Acid in Karst

by Simon Frank<sup>1</sup>, Nadine Goeppert<sup>2</sup>, and Nico Goldscheider<sup>2</sup>

## Abstract

The monitoring of water quality, especially of karst springs, requires methods for rapidly estimating and quantifying parameters that indicate contamination. In the last few years, fluorescence-based measurements of tryptophan and humic acid have become a promising tool to assess water quality in near real-time. In this study, we conducted comparative tracer tests in a karst experimental site to investigate the transport properties and behavior of tryptophan and humic acid in a natural karst aquifer. These two tracers were compared with the conservative tracer uranine. Fluorescence measurements were conducted with an online field fluorometer and in the laboratory. The obtained breakthrough curves (BTCs) and the modeling results demonstrate that (1) the online field fluorometer is suitable for real-time fluorescence measurements of all three tracers; (2) the transport parameters obtained for uranine, tryptophan, and humic acid are comparable in the fast flow areas of the karst system; (3) the transport velocities of humic acid are slower and the resulting residence times are accordingly higher, compared to uranine and tryptophan, in the slower and longer flow paths; (4) the obtained BTCs reveal additional information about the investigated karst system. As a conclusion, the experiments show that the transport properties of tryptophan are similar to those of uranine while humic acid is partly transported slower and with retardation. These findings allow a better and quantitative interpretation of the results when these substances are used as natural fecal and contamination indicators.

## Introduction

To protect drinking water from contamination, the rapid estimation of water-quality parameters has become a major task. In the last few years, fluorescence-based measurements of tryptophan and humic substances have become a promising tool for the rapid assessment of bacterial and other organic contamination (Sorensen et al. 2015, 2018a; Frank et al. 2018). With this method, it is possible to locate contamination origin and to monitor

how contamination spreads through the karst aquifer network in near real-time (Ediriweera and Marshall 2010).

Dissolved humic substances in natural waters are mainly derived from dead and decaying soil detritus, aquatic plants and debris (Hongve 1999). Humic substances are heterogeneous molecular compounds resulting from abiotic and biotic reactions in soil (Piccolo et al. 2018). The presence of humic acid in water can have a significant adverse impact on the treatability of that water and decreases the success of disinfection processes (Oliver 1983).

Tryptophan is a fluorescent amino acid containing an amino group, a carboxylic acid group and a side chain indole. Tryptophan is essential for humans and is used in the biosynthesis of proteins. Tryptophan is often used as an indicator of biological activity (Maie et al. 2003; Fellmann et al. 2010). Determann et al. (1998) and Quiers et al. (2014) showed that tryptophan-like fluorescence is directly related to microbial activity of bacteria, and Sorensen et al. (2015) demonstrated that it can be used to investigate the biological quality of drinking water.

So far, several studies use dissolved tryptophan and humic substances as indicators of water quality (e.g., Cumberland et al. 2012; Baker et al. 2015; Sorensen

<sup>1</sup>Corresponding author: Institute of Applied Geosciences, Division of Hydrogeology, Karlsruhe Institute of Technology (KIT), Kaiserstr. 12, 76131 Karlsruhe, Germany; simon.frank@kit.edu

<sup>2</sup>Institute of Applied Geosciences, Division of Hydrogeology, Karlsruhe Institute of Technology (KIT), Kaiserstr. 12, 76131, Karlsruhe, Germany

*Article impact statement:* This research presents a comparison of the transport behavior of uranine, tryptophan and humic acid derived from tracer tests.

Received October 2019, accepted May 2020.

© 2020 The Authors. *Groundwater* published by Wiley Periodicals, Inc. on behalf of National Ground Water Association.

This is an open access article under the terms of the Creative Commons Attribution License, which permits use, distribution and reproduction in any medium, provided the original work is properly cited.

doi: 10.1111/gwat.13015

et al. 2018b), however, the behavior and transport properties of these substances with respect to flow velocities, residence times and especially degradation processes are still insufficiently known, although they are crucial to accurately determine organic contamination, especially at fast reacting karst springs.

To determine these relevant parameters, we conducted a tracer test, comparing tryptophan and humic acid to the conservative tracer uranine in a well-studied karst experimental site. The fluorescent dye uranine is commonly used as an almost ideal conservative tracer because of its low detection limit and favorable properties (Käss 2004).

Generally, tracer tests are powerful tools to study groundwater flow and contaminant migration, especially in karst systems (Goepfert and Goldscheider 2008). Artificial tracers have been applied in the identification of recharge areas, flow directions and velocities and groundwater vulnerability (Käss 2004; Massei et al. 2006; Goldscheider 2008) and to characterize transport processes in natural streams (Boulton et al. 2010; Lemke et al. 2013). Numerous mathematical models have been developed to estimate transport parameters from the observed breakthrough curves (BTCs, e.g., Kreft and Zuber 1978; Maloszewski et al. 1992; Berkowitz et al. 2006).

In this study, we compared tryptophan and humic acid with the conservative tracer uranine in a pristine karst experimental site in the Austrian Alps, in order to identify differences between the ideal conservative tracer and the two natural organic compounds that were used as artificial tracers in this study. We determined flow velocities, residence times, dispersion and retardation of tryptophan and humic acid in a natural karst groundwater system during different hydrological conditions in order to achieve a better understanding of these two substances, which is important with respect to their utilization as water quality indicators. Additionally, we compared novel fluorescence-based online field measurements and conventional laboratory analyses of water samples in order to test and evaluate the near real-time detection and quantification of tryptophan and humic acid by means of field instruments.

## Materials and Methods

### Study Site

A well-investigated small-scale epikarst system representing a model karst aquifer that can be used as an ideal experimental site for field-scale tracer tests was chosen as test site (Goepfert and Goldscheider 2019). The karst system is located west of Lake Formarin in Western Austria (Figure 1a) and consists of a swallow hole, where the three tracers were injected, and a downstream spring that served as monitoring and sampling site (Figure 1b). At high-flow conditions, an overflow spring exists between the swallow hole and the sampling point (Figure 1b). The catchment area consists of

highly karstified limestone (Plattenkalk Formation) and the spring can be characterized as a typical epikarst spring with shallow flow paths between the swallow hole and the outlet. The main advantages of this study area for the conducted comparative tracer tests are:

- short distances (linear distance between the injection point and the spring outlet is 235 m) and relatively high flow velocities resulting in short experiment durations
- relatively simple hydrogeological conditions with an active swallow hole connected to a perennial karst spring
- low and constant background concentrations of tryptophan and humic substances at the spring
- good accessibility of the study site

These advantages make this study area an ideal site for the evaluation of the transport properties of different substances in groundwater.

The injection and monitoring for the first test series were done from August 16 to 18, 2017 under the same conditions for all three tracers, with direct injection of the dissolved tracers into flowing water and constant spring discharge between 29 and 31 L/s (mean to high flow) during the monitoring period. The second test series was conducted from September 7 to 9, 2017 with constant discharge conditions between 7.5 and 8.5 L/s (low-flow conditions). A third test with uranine and tryptophan was conducted from July 6 to 7, 2017 under low to mean flow conditions (discharge between 14 and 14.5 L/s). To compare the three tracers, within each test series, water samples were taken manually and analyzed in the laboratory. An online field fluorimeter (FF) was used for each test series, to test its applicability to detect and to measure the three tracers in real time and in higher resolution.

### Used Tracers

Uranine (AppliChem GmbH, Darmstadt, Germany), L-Tryptophan (Sigma-Aldrich/Merck KGaA, Darmstadt, Germany), and humic acid (as Humic Acid sodium salt, Sigma-Aldrich/Merck KGaA) were used as tracers. The structural formulas, the solubility in water and the main optical properties of the three tracers are given in Table 1.

Uranine shows the strongest fluorescence of all fluorescence tracers (Käss 2004). The detection limit of uranine is extremely low ( $\sim 0.005 \mu\text{g/L}$ ); its solubility is very high, and it is harmless for the environment (Behrens et al. 2001). Therefore, uranine is widely used for hydrogeological tracer tests.

L-Tryptophan is an aromatic, proteinogenic amino-acid with a carboxylic acid group and a side chain indole and is one of three fluorescent amino acids. The fluorescence properties of tryptophan are used to investigate the dynamics of dissolved natural organic material (Wagner 2014).

Humic substances have a polymeric composition without a reproducible structure. They consist of aliphatic

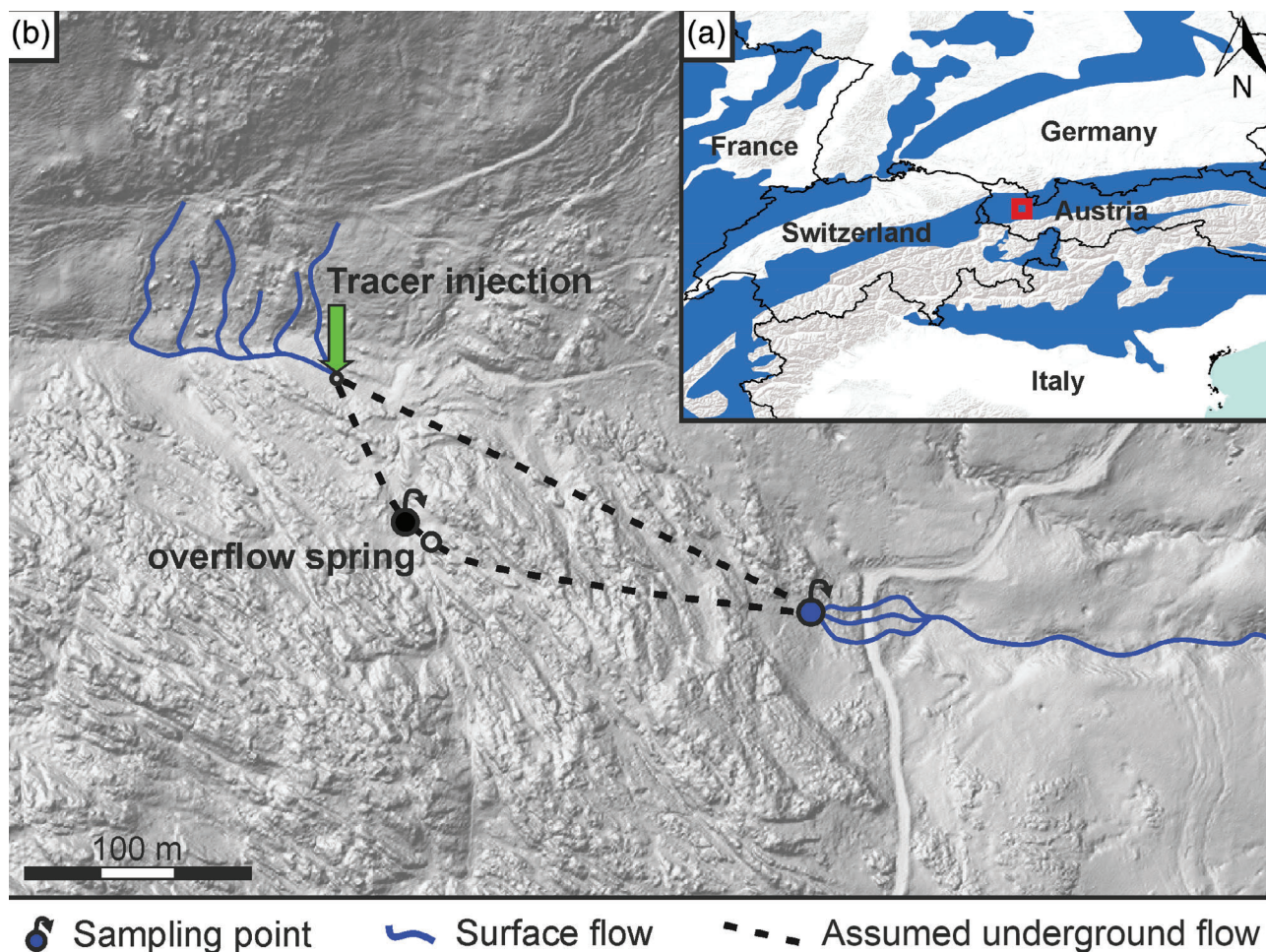


**Figure 1.** (a) Location of the test site in Western Austria (basemap: World Karst Aquifer Map; modified from Chen et al. [2017]); (b) detailed view of the karst experimental site (data from basemap: data.vorarlberg.gv.at).

and heterocyclic structures which give them the optical property of fluorescence (Sun et al. 2010). Humic substances are decomposition products of dead herbal and animal material which develop through biological conversion in soil and water. Depending on their origin, humic substances created in water have a smaller size and are generally younger than humic substances from soil. The fluorescence properties of humic substances are depending on the amount of aromatic structures and their actual size (Wagner 2014).

Because environmental conditions can have a complex influence on the characteristics of especially tryptophan and humic acid fluorescence (Chen and Kenny 2007; Sun et al. 2010), a comparative tracer test with uranine was conducted to determine the transport properties (transport velocities, residence times, dispersion and retardation) of the two used substances. Sorensen et al. (2018a, 2018b) used tryptophan as an indicator of fecal pollution and observed good correlation between dissolved tryptophan (tryptophan-like fluorescence) and thermotolerant coliforms, and Sorensen et al. (2016) demonstrated that the majority of the tryptophan-like fluorescence signal was within the  $<0.22\mu\text{m}$  size fraction.

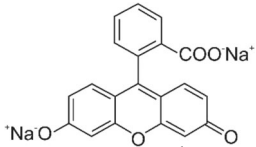
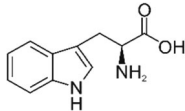
Therefore, for this study a tryptophan solution was used as tracer.

### Tracer Measurements

The three tracers were analyzed directly on site with an online field fluorometer (FF) GGUN-FL30 (Albillia Co., Neuchâtel, Switzerland) with optics for uranine, tryptophan and amino G acid. In addition, water samples were taken in 4 to 30 min intervals for analysis in the laboratory. All water samples were collected in 50 mL brown glass bottles and stored in the dark at  $4^\circ\text{C}$  until analysis. In the laboratory, uranine was measured with a LS55 fluorescence spectrometer (Perkin Elmer Inc., Waltham, Massachusetts) and tryptophan and humic acid were analyzed with the Aqualog fluorometer (Horiba Ltd., Kyoto, Japan). All samples were analyzed in a quartz cuvette with a path length of 10 mm maintained at a constant temperature of  $20^\circ\text{C}$ .

With the Aqualog, excitation-emission matrices (EEMs) were acquired by simultaneous scanning of the absorbance (excitation) and the fluorescence emission spectrum at each excitation wavelength. For the samples analyzed with the Aqualog, a simultaneous scan of excitation and emission wavelength from 240 to 600 nm

**Table 1**  
Structural Formula and Properties of the Three Used Tracers

	Uranine	L-Tryptophan	Humic Acid
Structural formula			Macromolecule without defined structural formula
Solubility (g/L) (H <sub>2</sub> O, 20 °C)	> 600 <sup>1</sup>	10 <sup>2</sup>	n.n.
Peak λ <sub>em</sub> (nm)	512 <sup>1</sup>	350 <sup>3</sup>	Peak 1:380-480 <sup>4</sup> Peak 2:420-480 <sup>4</sup>
Peak λ <sub>ex</sub> (nm)	491 <sup>1</sup>	280 <sup>3</sup>	Peak 1:250-260 <sup>4</sup> Peak 2:330-350 <sup>4</sup>

<sup>1</sup> Käss (2004).

<sup>2</sup> Römpf Enzyklopädie Online (2020).

<sup>3</sup> Lakowicz (2006).

<sup>4</sup> Parlanti et al. (2000).

with 5-nm intervals was performed. A deionized water blank was used to validate the performance of the instrument and to measure the signal-to-noise ratio. First and second order Rayleigh scattering was removed by nullifying the signal intensities of the Rayleigh lines. The Raman scatter line was removed by subtracting the blank from the sample EEM. EEMs were also corrected for inner filter effects (IFE) using the parallel absorbance measurement from the blank and from the sample, following the procedure of Gilmore (2011). To determine the fluorescence intensities (FIs), the peak-picking technique was used (Coble 1996). In accordance with Fellmann et al. (2010), the tryptophan peak was identified at excitation wavelength (λ<sub>ex</sub>) 270 to 280 nm and emission wavelength (λ<sub>em</sub>) between 330 and 370 nm. In the field, humic acid was determined using the amino G acid channel of the FF. In the EEM, it was identified at λ<sub>ex</sub> 320 to 375 nm and λ<sub>em</sub> 430 to 500 nm. 20 μL of a pH 10 buffer solution were added to the water samples analyzed for uranine (with LS55) and tryptophan (with Aqualog) to increase the fluorescence yield. Samples were not diluted.

### Modeling of the BTCs

To model the BTCs in this karst system (with major conduits), the commonly used advection-dispersion model (ADM, Kreft and Zuber 1978) was used:

$$C_f(x, t) = \frac{M}{Q \cdot t_0 \cdot \sqrt{4\pi \cdot P_D \cdot \left(\frac{t}{t_0}\right)^3}} \exp \left[ -\frac{\left[1 - \frac{t}{t_0}\right]^2}{4 \cdot P_D \cdot \frac{t}{t_0}} \right], \quad (1)$$

where  $C$  is the tracer concentration in the water (μg/L),  $M$  is the injected tracer mass (mg),  $Q$  is the discharge or pumping rate (m<sup>3</sup>/s),  $t_0$  is the mean flow time,  $P_D$  is the dispersion parameter (reciprocal Péclet number,  $P_D = D_L/(v \cdot x)$ ),  $t$  is a time variable (s),  $D_L$  is the

longitudinal dispersion coefficient ( $D_L = \alpha_L \cdot v$ ) (m<sup>2</sup>/s),  $v$  is the effective flow velocity  $v = x/t_0$  (m/s),  $x$  is the distance between injection and sampling point (m) and  $\alpha_L$  is the longitudinal dispersivity (m).

The observed BTCs during low-flow conditions show a more pronounced tailing compared to mean- to high-flow conditions. To model these BTCs a two-region nonequilibrium (2RNE) model (Field and Pinsky 2000) was used. This model accounts for exchange between mobile and immobile fluid regions in a karst system. Water in the immobile fluid region is assumed as stagnant relative to the water flowing in the mobile fluid region. Therefore, the advection-dispersion equation is extended by two parameters, a partitioning coefficient  $\beta$  between mobile and immobile fluid regions and a mass transfer coefficient  $\omega$  between the two regions. For simplification, only the dimensionless form is given here (modified after Field and Pinsky 2000; Toride et al. 1993).

$$\beta \frac{\partial C_1}{\partial T} = \frac{1}{Pe} \frac{\partial^2 C_1}{\partial Z^2} - \frac{\partial C_1}{\partial Z} - \omega(C_1 - C_2) \quad (2)$$

$$(1 - \beta) \frac{\partial C_2}{\partial T} = \omega(C_1 - C_2) \quad (3)$$

where  $C$  represents the dimensionless solute concentration and  $T$  and  $Z$  dimensionless time and space variables. The Péclet number  $Pe$  is defined by the model parameters mean flow velocity ( $v_m$ ) and dispersion coefficient  $D$ :

$$Pe = \frac{x v_m}{D} = \frac{x}{\alpha} \quad (4)$$

where  $x$  is the flow distance and  $\alpha$  the dispersivity. The dimensionless partitioning coefficient  $\beta$  ( $0 \leq \beta \leq 1$ ) indicates the proportion of mobile water, while the mass transfer coefficient  $\omega$  describes the exchange rate between the two fluid regions.

The 2RNE model was already successfully applied to the simulation of BTCs from tracer tests in karstic

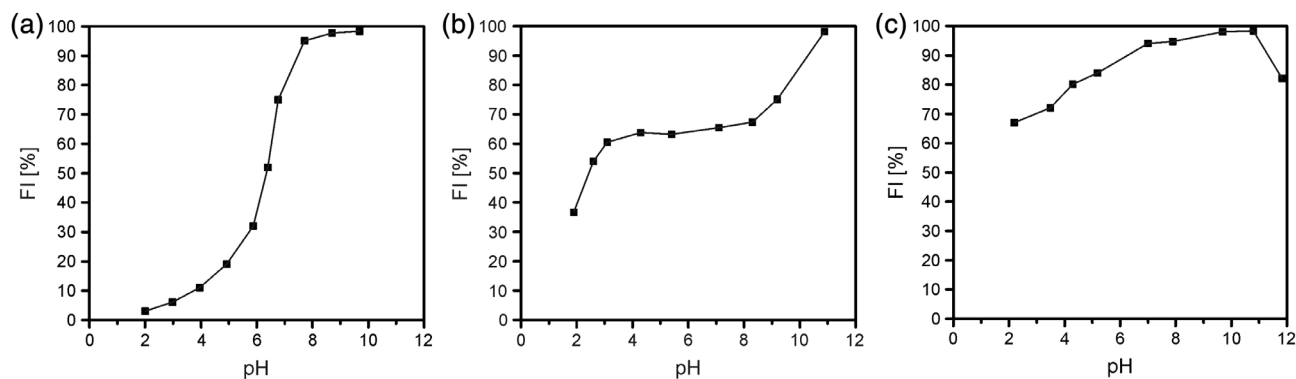


**Figure 2.** Dependency of the fluorescence intensity of the pH value for (a) uranine, (b) tryptophan, (c) humic acid; the highest measured fluorescence intensity was assumed as 100%.

and nonkarstic environments (e.g., Birk et al. 2005; Geyer et al. 2007; Lauber et al. 2014; Ender et al. 2018).

Because the observed BTCs of all three tracers show two individual peaks during mean- to high-flow conditions, both peaks were modeled separately according to the multidispersion model (MDM) from Maloszewski et al. (1992). The different peaks can be modeled by superposition of two or more ADMs (Seaman et al. 2007). For each peak,  $t_0$  and  $D$  have to be determined individually.

The modeling was done with the software package CXTFIT (Toride et al. 1999) where both, the ADM and the 2RNE model, are implemented.

### pH Dependence of Tracer Fluorescence

For all three tracers, a laboratory experiment was conducted to investigate the pH dependence of fluorescence. Diluted solutions were prepared from a stock solution (1 g/L) for each tracer. The pH adjustment was done by adding microliters of concentrated NaOH and HCl respectively. The pH reading was conducted with a WTW SenTix 940 sensor (Xylem Analytics Germany Sales GmbH & Co. KG, WTW, Weilheim, Germany). The FIs of all samples were measured at a constant temperature of 20°C with a LS55 fluorescence spectrometer (uranine) and an Aqualog fluorometer (tryptophan and humic acid). The fluorescence peaks were identified at the wavelength described aforementioned. The results of the fluorescence measurements at different pH values for all three tracers are given in Figure 2.

Uranine fluorescence is highly influenced by the pH; the highest FIs were measured at alkaline pH over 10, as also described in Käss (2004). Tryptophan also shows higher FI at alkaline pH, but the fluorescence is more or less constant in the pH range between 5 and 8 (Sun et al. 2010). The influence of the pH is also visible for humic acid, which shows higher fluorescence at alkaline values but is also more or less constant in the range 6 to 8. During the investigation period, the spring water had constant pH between 7.8 and 8.0.

## Results and Discussion

### Comparison of Field and Laboratory Measurements

A comparison of the measured uranine concentrations with the LS55 and the FF gives a satisfying consistency, with an  $R^2$  of 0.995 and  $a = 0.960$  (Figure A1a). For tryptophan, comparison of the measured concentrations with the Aqualog in the laboratory and the FF shows an  $R^2$  value of 0.98 and  $a = 1.003$  which also indicates a satisfying consistency (Figure A1b). For humic acid, comparison between the laboratory and online measurements indicate a good performance of the FF with an  $R^2$  of 0.97 and  $a = 0.995$  (Figure A1c), slightly lower than for uranine and tryptophan.

The measurement of an uranine sample with the Aqualog produced an EEM that reveals the maximum fluorescence at  $\lambda_{ex}$  490 nm and  $\lambda_{em}$  of 515 nm (Figure 3a). The EEM scan also shows a secondary fluorescence maximum at  $\lambda_{ex}$  320 nm (Figure 3a).

The produced EEM spectrum for Tryptophan shows a clearly identifiable peak at  $\lambda_{ex}$  between 270 and 280 nm and  $\lambda_{em}$  between 330 and 370 nm (Figure 3b), which is very similar to other studies (e.g., Coble 1996; Fellmann et al. 2010).

The produced EEM spectrum for humic acid sodium salt shows more than one identifiable peak (Figure 3c). The excitation and emission wavelengths where the peak was identified in this study with the Aqualog were  $\lambda_{ex}$  320 to 350 nm and  $\lambda_{em}$  400 to 480 nm (according to Coble 1996; Parlanti et al. 2000). To identify the humic acid with the FF, the channel for amino G acid was used, which is at a similar wavelength than the one used from the EEMs.

### BTCs and Obtained Transport Parameters

To obtain high-resolution results, the BTCs for all test series (mean- to high-flow, low- to mean-flow, and low-flow) were produced from the FF data that were also used for modeling. During mean- to high-flow, uranine was first detected 22 min after the injection and reached a maximum of 20.1  $\mu\text{g/L}$  after 32 min (Figure 4a). The BTC shows a second peak after 63 min with a concentration of 4.2  $\mu\text{g/L}$ . The total recovery was 74%

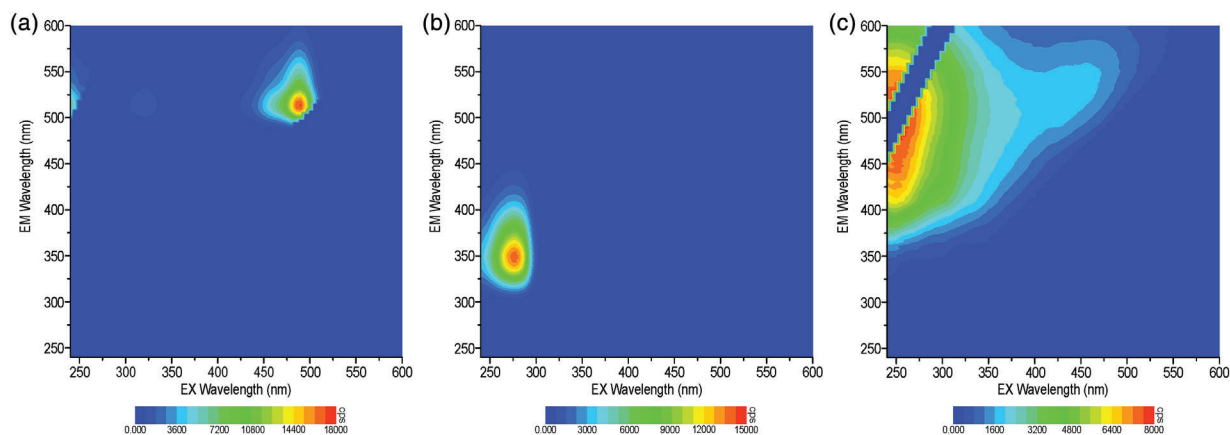


**Figure 3.** (a) EEM spectra of uranine recorded with the Aqualog, which shows  $\lambda_{ex}$  and  $\lambda_{em}$  of the main and secondary uranine fluorescence peak; (b) EEM spectra of tryptophan, which shows the main tryptophan fluorescence peak; (c) EEM spectra of humic acid.

which indicates that the monitored spring is the major outlet of the system, but infiltration into deeper parts of the aquifer also occurs. This conclusion is supported by other tracer tests performed in this system (Goepfert and Goldscheider 2019).

An explanation of the observed multiplexes and tailing effects could be different flow-paths with different lengths, dispersivities, and flow velocities (Goldscheider et al. 2008). The overflow spring (Figure 1b), which is only active during high-flow conditions at the main spring (>25 L/s), indicates the existence of at least a secondary flow path.

The observed BTC for tryptophan (Figure 4b) has an almost identical shape compared to the uranine BTC. Tryptophan was first detected 22.5 min after injection and reached a maximum concentration of 80.4  $\mu\text{g/L}$  after 32 min. Again, the BTC shows a second peak after 62.5 min with a concentration of 15.3  $\mu\text{g/L}$ . The calculated total recovery of tryptophan was 70.6%, slightly lower than for uranine.

Although the recovery rates of uranine and tryptophan are comparable, additional processes in the aquifer, such as degradation and sorption, can occur. Some studies found for example, that bacteria were able to degrade aromatic amino acids (Janke 1950; Akujkar et al. 2014), which might be a possible explanation for the slightly lower recovery, although it is quite unlikely that these processes occur in the investigated system because of the short transit times, high flow velocities, and short distances.

The BTC of humic acid again shows two distinct peaks: the first occurs after 33 min with a maximum concentration of 1373.0  $\mu\text{g/L}$ , while the second peak was recorded after 78 min with a concentration of 218.4  $\mu\text{g/L}$  (Figure 4c). This is a delay of about 15 min compared to uranine and tryptophan. The shape of the first peak is similar to uranine and tryptophan, while the second peak is flatter and wider compared to the other two tracers. The total recovery of humic acid is 76%, which is slightly higher compared to uranine and tryptophan.

The second test series was conducted in the same system during low-flow conditions. The results show BTCs for all three tracers with only one identifiable peak (Figure 5) which show a more pronounced tailing compared to the BTCs observed during high-flow conditions. The modeling for these BTCs was done with a 2RNE model.

During low-flow, uranine was first detected 59.5 min after the injection and reached a maximum of 24.8  $\mu\text{g/L}$  after 89 min (Figure 5a). These observed time values are 2.7 times higher compared to high-flow conditions. The total recovery was 60.8% which is lower than during high-flow and also indicates that the monitored spring is the major outlet of the system, but infiltration into deeper parts of the aquifer also occurs.

The observed BTC for tryptophan (Figure 5b) has an almost identical shape compared to the uranine BTC. Tryptophan was first detected 60.5 min after injection and reached a maximum concentration of 99.2  $\mu\text{g/L}$  after 90.5 min. This is again 2.7 times more compared to low-flow conditions. The calculated total recovery of tryptophan was 59.7%, slightly lower than that for uranine.

The recovery rates of uranine and tryptophan are also comparable during low-flow conditions, but additional processes in the aquifer, such as degradation and sorption, can occur and cannot be excluded. Compared to high-flow conditions, the transit times are higher and the resulting flow velocities are lower.

The BTC of humic acid shows a similar shape compared to uranine and tryptophan (Figure 5c). Humic acid was first detected 65 min after injection and the peak occurred after 92.5 min with a concentration of 1885  $\mu\text{g/L}$ . This is a slight delay compared to uranine and tryptophan. The total recovery of humic acid is 60.5%, which is in a similar range as the other two tracers. The partitioning coefficient  $\beta$  is between 0.77 for uranine and 0.68 for humic substances. This means that between two-thirds and three-quarters of the water can be considered as mobile.

A third tracer test was conducted with uranine and tryptophan during low to mean discharge conditions (14.5

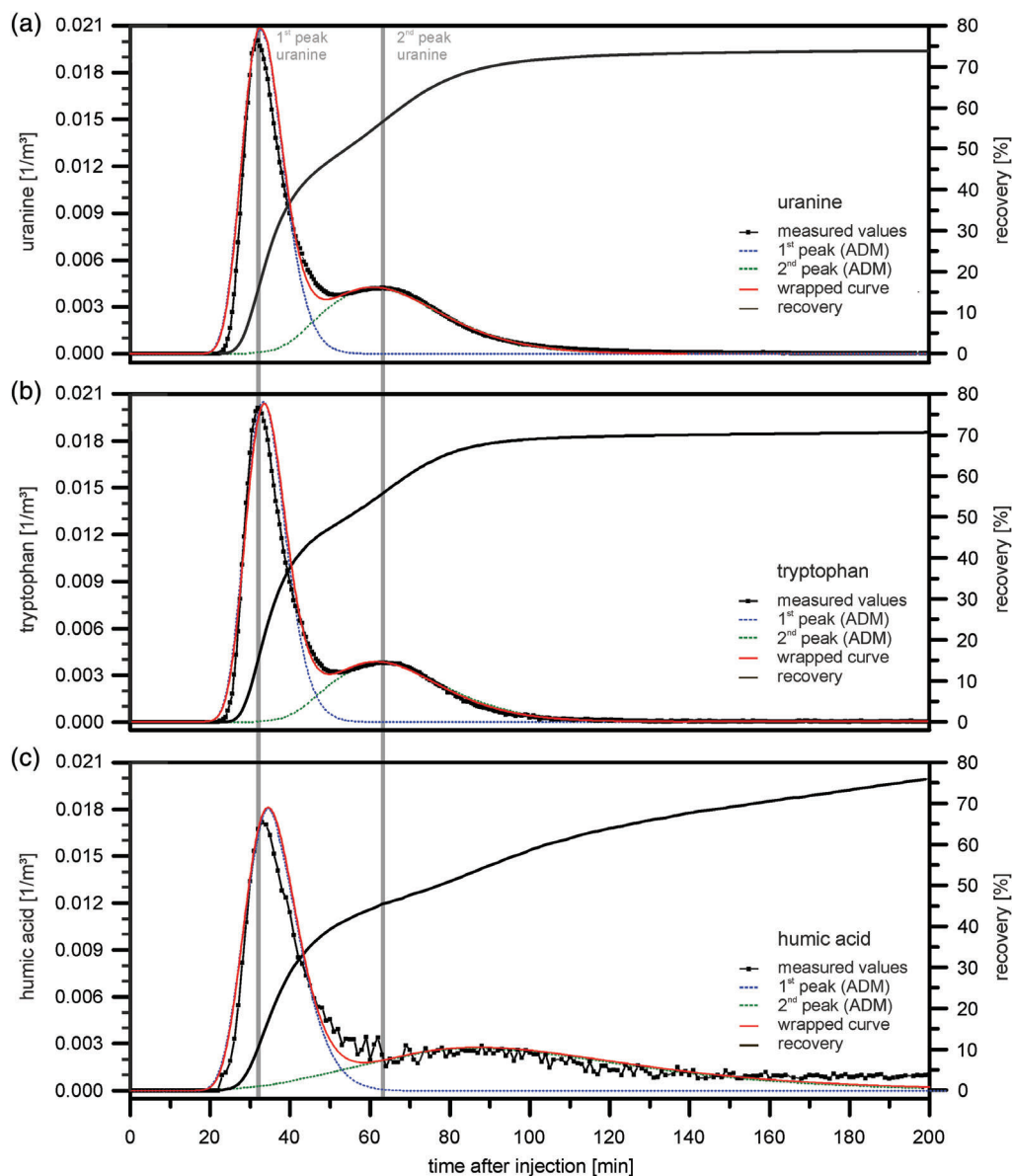


**Figure 4.** BTCs during mean- to high-flow conditions of (a) uranine, (b) tryptophan, (c) humic acid, each time together with the recovery and the modeled BTC for both peaks and the wrapped curve. Concentrations are normalized (c/M).

and 14 L/s respectively). The BTCs show only one peak with a similar shape compared to the curves obtained during low-flow conditions. The obtained values for uranine and tryptophan are also comparable. The BTCs, modeled BTCs, recovery rates and the corresponding data are given in Figure A2 and Table 2.

Table 2 gives an overview of all parameters obtained from the three tracer tests.

During mean- to high-flow conditions, the time of first detection ( $t_1$ ),  $t_p$  and the corresponding  $v_{\max}$  and  $v_p$  for the first tracer peak, are comparable for all three tracers. The modeled parameters  $v$ ,  $t_0$  and longitudinal dispersion ( $D$ ) were determined for both peaks for the conservative tracer uranine. The retardation factor was set to 1.0. The determined values for  $v$  and  $t_0$  for uranine were used as fixed input parameters for the modeling of the other two tracers. While the mean transit time is

comparable for uranine and tryptophan, the mean transit time for the second peak of humic substances is about 20% higher compared to the other two tracers. The modeled retardation factor for the secondary humic acid peak is 1.5 compared to uranine (1.0 = no retardation).

During low-flow conditions,  $t_1$ ,  $t_p$  and the corresponding velocities  $v_{\max}$  and  $v_p$  are comparable for all three tracers with a slight delay and slightly lower velocities for humic substances. To determine retardation, the same procedure as during high-flow was applied. Compared to uranine and tryptophan, a retardation factor of 1.11 was determined for humic substances.

Retardation processes seem to have no influence on tryptophan because the modeled retardation factor is also 1.0 for both peaks during high-flow and for the BTC during low-flow (like the conservative uranine). Retardation seems to have a larger influence on the humic

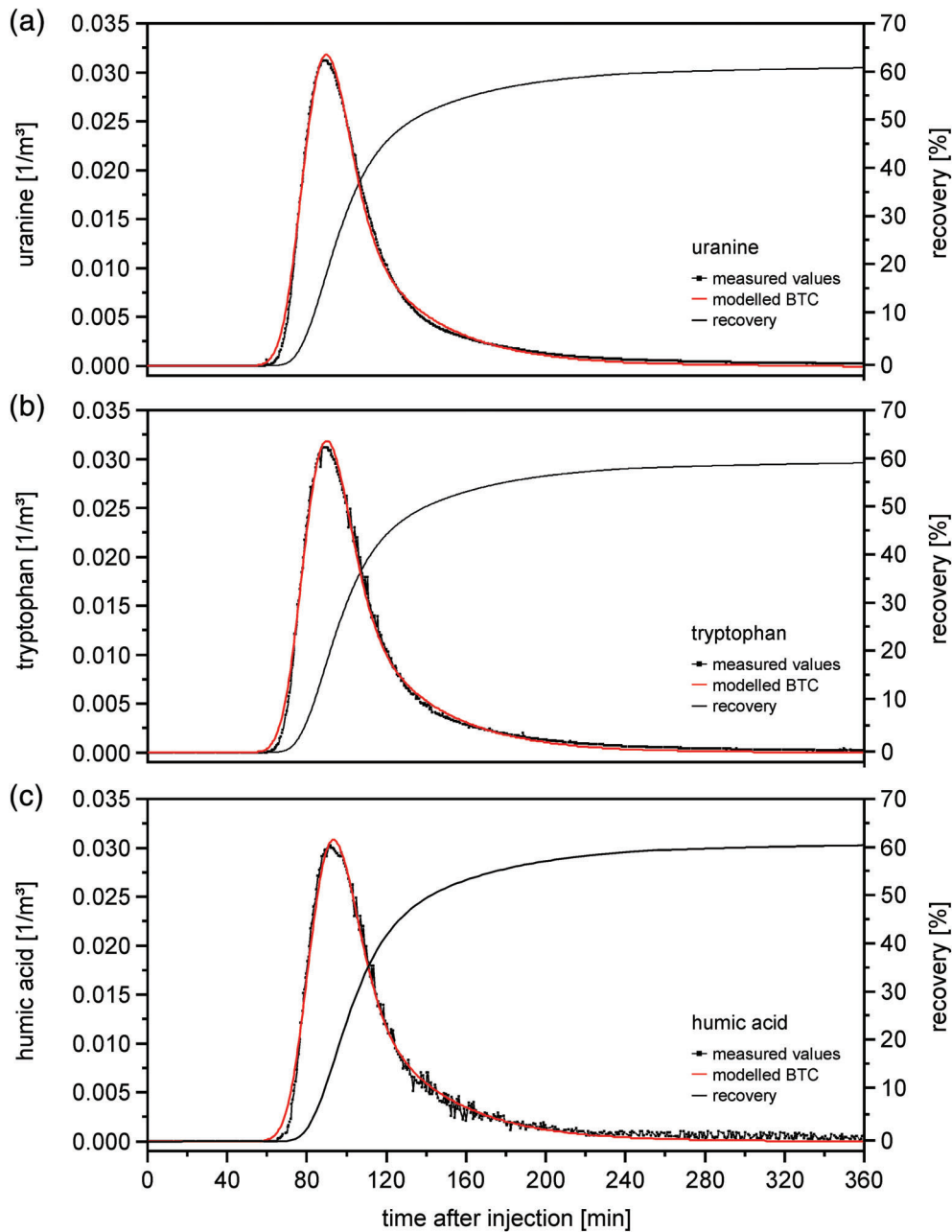


**Figure 5.** BTCs during low-flow conditions of (a) uranine, (b) tryptophan, (c) humic acid, each time together with the recovery and the modeled BTC.

acid tracer, especially on the second peak during high-flow but it is also visible during low-flow.

Because uranine can be considered as an almost ideal conservative tracer, the slower transport of humic acid can be attributed to a reactive transport behavior of the humic substances. For these kinds of substances, adsorption and desorption processes are of particular importance. Because of the higher flow velocities in the main flow path during mean- to high-flow (one major conduit), these factors are almost negligible. Factors influencing the retardation are different surface conditions and different properties of the aquifer material (Aklujkar et al. 2014), which play a more important role in the secondary flow path, which is longer, more diffuse and the transport occurs slower.

The blurrier peak in the EEM spectrum of humic acid apparently also leads to a more blurred signal in the FF, which might also influence the shape of the humic acid BTC. The tracers uranine and tryptophan produce a clear fluorescence signal which can be seen in the smooth BTCs of these two tracers (Figure 3a and 3b). In comparison to this, the humic acid FF signal is associated with a certain degree of variation, especially at lower concentrations.

## Conclusion

Given the importance of real time water quality indicators, many studies use tryptophan as fecal indicator (e.g., Sorensen et al. 2015; Frank et al. 2018) and humic

**Table 2**  
**Overview of the obtained and calculated transport parameters for all three test series**

Symbol	Unit	Mean to High Flow (ADM/MDM)						Low- to Mean Flow <sup>1</sup> (2RNE)			Low Flow (2RNE)		
		Uranine		Tryptophan		Humic Acid		Uranine	Tryptophan	Humic Acid	Uranine	Tryptophan	Humic Acid
		First Peak	Second Peak	First Peak	Second Peak	First Peak	Second Peak						
<b>Experimental conditions</b>													
M	g	1.0		4.0		80.0		0.8	3.2	0.8	3.2	65	
Q	L/s	30		31		29		14.5	14.0	8.5	7.5	7.5	
<b>Basic parameters</b>													
$t_1$	min	22.0		22.5		23.0		57.5	58.0	59.5	60.5	65.0	
$t_p$	min	32.0	63.0	32.0	62.5	33.0	78.0	81.5	81.5	89.0	90.5	92.5	
$C_p$	µg/L	20.1	4.2	80.4	15.3	1372.9	218.4	20.8	101.0	24.8	99.2	1885	
Normalized peak concentration	$m^{-3}$	0.020	0.004	0.020	0.004	0.017	0.003	0.038	0.032	0.031	0.031	0.029	
Maximum velocity	m/min	10.7		10.4		10.2		4.1	4.1	3.9	3.9	3.6	
Peak velocity	m/min	7.3	3.8	7.3	3.8	7.1	3.0	2.9	2.9	2.6	2.6	2.5	
Recovery	%	73.9		70.6		76.1		69.1	67.8	60.8	59.7	60.5	
<b>Modeled parameters</b>													
Coefficient of determination		0.98		0.98		0.96		0.98	0.98	0.99	0.99	0.99	
Mean flow velocity	m/min	7.0	3.5	7.0	3.5	7.0	3.5	2.6	2.6	2.4	2.4	2.4	
Mean transit time	min	33.6	67.1	33.6	67.1	33.6	67.1	90.4	90.4	97.9	97.9	97.9	
Partitioning coefficient		—	—	—	—	—	—	0.83	0.81	0.78	0.76	0.70	
Transfer coefficient		—	—	—	—	—	—	1.05	1.01	1.12	1.06	1.01	
Longitudinal dispersion	$m^2/min$	15.7	23.7	15.7	23.7	15.7	23.7	6.2	6.2	5.0	5.0	5.0	
Retardation factor	—	1.00	1.00	1.00	1.00	1.03	1.48	1.00	1.00	1.00	1.00	1.11	

Bold numbers indicate fixed values during modeling.  
<sup>1</sup> BTCs and modeled BTCs are shown in Figure A2.

substances as contaminant vector. There is the need to enhance the knowledge about the transport behavior of these two substances.

In this study, we conducted three tracer tests in a karst experimental site, where we compared the transport of tryptophan and humic acid with the conservative tracer uranine. The main conclusions can be summarized as follows:

- Tracer test results show that modern online field fluorimeters can be used to measure fluorescence of tryptophan and humic acid in near real-time and in high resolution.
- The transport parameters obtained for the conservative tracer uranine and tryptophan, especially the flow velocities, transit times, and dispersion, are almost identical. The recovery rates of uranine and tryptophan are also comparable. All three tracer tests indicate that no reduction or retardation occurs in the investigated flow system for dissolved tryptophan.
- However, humic acid is transported slower compared to uranine and tryptophan. Therefore, the calculated and modeled transport parameters of humic substances are different. In this case, retardation occurs. The retardation factors for humic substances (between 1.1 and 1.5 in our study) indicate that sorption processes have a distinct influence on humic substances.

The tracer test also led to a better understanding of the investigated aquifer. During mean- to high-flow conditions, the BTCs of all three tracers show two clearly identifiable peaks, which indicate at least two flow paths. This was also verified with subsequent tracer tests

conducted in this system and is dependent on the discharge of the spring. At low-flow conditions only one flow path is active and the resulting BTCs have only one peak.

The observed and calculated transport parameters (residence time, mean flow-velocity, retardation) in the investigated system, lead to the conclusion that tryptophan behaves like a conservative tracer without retardation and reduction, at least in fast-flowing karst aquifer systems. On the other hand, this study also shows that humic substances undergo no reduction in fast-flowing areas, but reduction and retardation occur in slower flow-paths.

Therefore, these results can contribute to a better and quantitative interpretation when these two substances are used as fecal and contamination indicators.

## Acknowledgments

The study was funded by the European Commission through the FP7 Marie Curie CIG grant IMKA (grant agreement number 303837). We acknowledge support by the KIT-Publication Fund of the Karlsruhe Institute of Technology and special thanks are given to KIT laboratory staff Daniela Blank, Christine Buschhaus, and Christine Roske-Stegemann and our students Christian Arps, Timo Roth, Eva Häußler, and Lois Dufour for their help during fieldwork. The authors also thank Chloé Fandel for proofreading the original manuscript.

## Authors' Note

The authors do not have any conflicts of interest or financial disclosures to report.

## Appendix

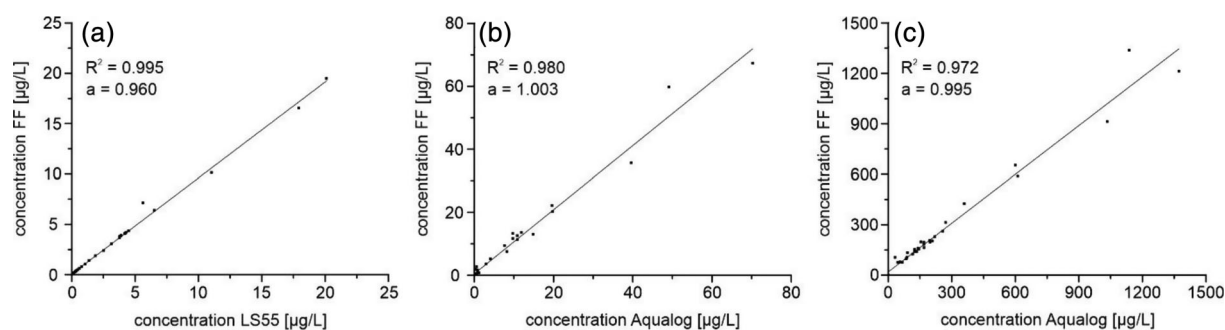


**Figure A1.** (a) Measured uranine concentration with the FF, compared to the measured concentration with the LS55 in the laboratory, (b) comparison of the measured tryptophan concentration of the FF and the Aqualog, and (c) comparison of the measured humic acid concentration with the FF and the Aqualog.

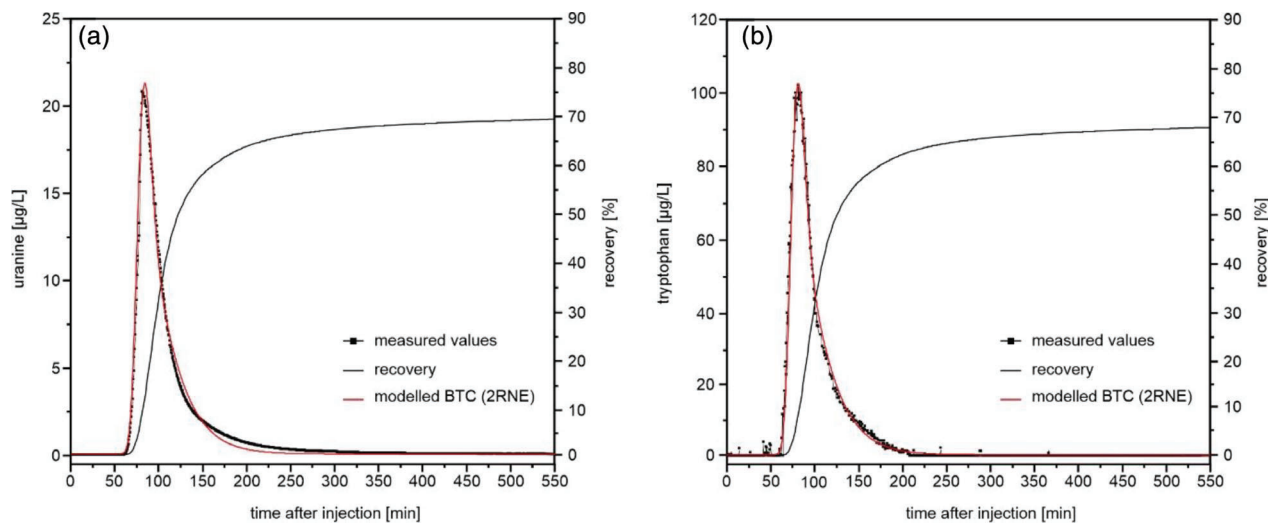


**Figure A2.** (a) BTC and recovery for uranine, discharge 14.5 L/s and (b) BTC and recovery of tryptophan, discharge 14 L/s.

## References

- Aklujkar, M., C. Risso, J. Smith, D. Beaulieu, R. Dubay, L. Giloteaux, C. DiBurro, and D. Holmes. 2014. Anaerobic degradation of aromatic amino acids by the hyperthermophilic archaeon *Ferroplasma acidophilum*. *Microbiology* 160: 2694–2709.
- Baker, A., S.A. Cumberland, C. Bradley, C. Buckey, and J. Bridgeman. 2015. To what extent can portable fluorescence spectroscopy be used in the real-time assessment of microbial water quality? *Science of the Total Environment* 532: 14–19.
- Behrens, H., U. Beims, H. Dieter, G. Dietze, T. Eikmann, T. Grummt, H. Hanisch, H. Henseling, W. Käß, H. Kerndorff, C. Leibundgut, U. Müller-Wegener, I. Rönnefahrt, B. Scharenberg, R. Schleyer, W. Schloz, and F. Tilkes. 2001. Toxicological and ecotoxicological assessment of water tracers. *Hydrogeology Journal* 9: 321–325.
- Berkowitz, B., A. Cortis, M. Dentz, and H. Scher. 2006. Modeling non-Fickian transport in geological formations as a continuous time random walk. *Reviews of Geophysics* 44, no. 2, 1–49.
- Birk, S., T. Geyer, R. Liedl, and M. Sauter. 2005. Process-based interpretation of tracer tests in carbonate aquifers. *Groundwater* 43: 381–388.
- Boulton, A.J., T. Datry, T. Kasahara, M. Mutz, and J.A. Stanford. 2010. Ecology and management of the hyporheic zone: Stream-groundwater interactions of running waters and their floodplains. *Journal of the North American Benthological Society* 29: 26–40.
- Chen, Z., A.U. Auler, M. Bakalowicz, D. Drew, F. Griger, J. Hartmann, G. Jiang, N. Moosdorf, A. Richts, Z. Stevanovic, G. Veni, and N. Goldscheider. 2017. The world karst aquifer mapping project: Concept, mapping procedure and map of Europe. *Hydrogeology Journal* 25, no. 3: 771–785.
- Chen, H., and J.E. Kenny. 2007. A study of pH effects on humic substances using chemometric analysis of excitation-emission matrices. *Annals of Environmental Science* 1: 1–9.
- Coble, P.G. 1996. Characterization of marine and terrestrial DOM in seawater using excitation emission matrix spectroscopy. *Marine Chemistry* 51: 325–346.
- Cumberland, S., J. Bridgeman, A. Baker, M. Sterling, and D. Ward. 2012. Fluorescence spectroscopy as a tool for determining microbial quality in potable water applications. *Environmental Technology* 33, no. 6: 687–693.
- Determann, S., J.M. Lobbes, R. Reuter, and J. Rullkötter. 1998. Ultraviolet fluorescence excitation and emission spectroscopy of marine algae and bacteria. *Marine Chemistry* 62: 137–156.
- Ediriweera, D.D., and I.W. Marshall. 2010. Monitoring water distribution systems: Understanding and managing sensor networks. *Drinking Water Engineering and Science* 3: 107–113.
- Ender, A., N. Goepfert, and N. Goldscheider. 2018. Spatial resolution of transport parameters in a subtropical karst conduit system during dry and wet seasons. *Hydrogeology Journal* 26: 2241–2255.
- Fellmann, J.B., E. Hood, and R.G.M. Spencer. 2010. Fluorescence spectroscopy opens new windows into dissolved organic matter dynamics in freshwater ecosystems: A review. *Limnology and Oceanography* 55: 2452–2462.
- Field, M.S., and P.F. Pinsky. 2000. A two-region nonequilibrium model for solute transport in solution conduits in karstic aquifers. *Journal of Contaminant Hydrology* 44, no. 3–4: 329–351.
- Frank, S., N. Goepfert, and N. Goldscheider. 2018. Fluorescence-based multi-parameter approach to characterize dynamics of organic carbon, faecal bacteria and particles at alpine karst springs. *Science of the Total Environment* 615: 1446–1459.
- Geyer, T., S. Birk, T. Licha, R. Liedl, and M. Sauter. 2007. Multitracer test approach to characterize reactive transport in karst aquifers. *Groundwater* 45: 36–45.
- Gilmore, A.M. 2011. Water-Quality Measurements with the HORIBA Jobin Yvon Aqualog, Technical Report, 11. Horiba Scientific.
- Goepfert, N., and N. Goldscheider. 2019. Improved understanding of particle transport in karst groundwater using natural sediments as tracers. *Water Research* 166: 115045.
- Goepfert, N., and N. Goldscheider. 2008. Solute and colloid transport in karst conduits under low- and high-flow conditions. *Groundwater* 46: 61–68.
- Goldscheider, N. 2008. A new quantitative interpretation of the long-tail and plateau-like breakthrough curves from tracer tests in the artesian karst aquifer of Stuttgart, Germany. *Hydrogeology Journal* 16, no. 7: 1311–1317.
- Goldscheider, N., J. Meiman, M. Pronk, and C. Smart. 2008. Tracer tests in karst hydrogeology and speleology. *International Journal of Speleology* 37, no. 1: 27–40.
- Hongve, D. 1999. Production of dissolved organic carbon in forested catchments. *Journal of Hydrology* 224: 91–99.

- Janke, A. 1950. Der mikrobielle Abbau von Aminosäuren. *Archiv für Mikrobiologie* 15: 472–499.
- Käss, W. 2004. *Geohydrologische Markierungstechnik*. Gebrüder Bornträger, Berlin, Stuttgart: Lehrbuch der Hydrogeologie.
- Kreft, A., and A. Zuber. 1978. On the physical meaning of the dispersion equation and its solution for different initial and boundary conditions. *Chemical Engineering Science* 33: 1471–1480.
- Lakowicz, J.R. 2006. *Principles of Fluorescence Spectroscopy*, 3rd ed. New York: Springer Science + Business Media.
- Lauber, U., W. Ufrecht, and N. Goldscheider. 2014. Spatially resolved information on karst conduit flow from in-cave dye tracing. *Hydrology and Earth System Sciences* 18: 435–445.
- Lemke, D., P.-A. Schnegg, M. Schwientek, K. Osenbrück, and O.A. Cirpka. 2013. On-line fluorometry of multiple reactive and conservative tracers in streams. *Environmental Earth Sciences* 69: 349–358.
- Maie, N., H.Q. Wang, J.P. Dupont, J. Rodet, and B. Laignel. 2003. Composition of a protein-like fluorophore of DOM in coastal wetland and estuarine ecosystems. *Water Research* 41: 563–570.
- Maloszewski, P., R. Benischke, and T. Harum. 1992. Mathematical modelling of tracer experiments in the karst of Lurbach-system. *Beitr. z. Hydrogeologie* 43: 116–136.
- Massei, N.H., Q. Wang, M.S. Field, J.P. Dupont, M. Bakalowicz, and J. Rodet. 2006. Interpreting tracer breakthrough tailing in a conduit-dominated karst aquifer. *Hydrogeology Journal* 14, no. 6: 849–858.
- Oliver, B.G. 1983. Dihaloacetonitriles in drinking water: Algae and fulvic acid as precursors. *Environmental Science & Technology* 17, no. 2: 80–83.
- Parlanti, E., K. Wörz, L. Geoffroy, and M. Lamotte. 2000. Dissolved organic matter fluorescence spectroscopy as a tool to estimate biological activity in a coastal zone submitted to anthropogenic inputs. *Organic Geochemistry* 31, no. 12: 1765–1781.
- Piccolo, A., R. Spaccini, M. Drosos, G. Vinci, and V. Cozzolino. 2018. The molecular composition of humus carbon: Recalcitrance and reactivity in soils, the future of soil carbon. *Its Conservation and Formation*: 1, 87–124.
- Quiers, M., C. Batiot-Guilhe, C.C. Bicalho, Y. Perrette, J.-L. Seidel, and S. Van Exter. 2014. Characterization of rapid infiltration flows and vulnerability in a karst aquifer using a decomposed fluorescence signal of dissolved organic matter. *Environmental Earth Sciences* 71: 553–561.
- Römpf Enzyklopädie Online. 2020. Abschnitte: Aminosäuren, Biologische Abbaubarkeit, Huminstoffe, Phenylalanin, Proteine, Tryptophan, Uranin. [www.roempp.com](http://www.roempp.com) (accessed March 18, 2020).
- Seaman, J.C., P.M. Bertsch, M. Wilson, J. Singer, F. Majas, and S.A. Aburime. 2007. Tracer migration in a radially divergent flow field: Longitudinal dispersivity and anionic tracer retardation. *Vadose Zone Journal* 6, no. 2: 373–386.
- Sorensen, J.P.R., A. Baker, S.A. Cumberland, D.J. Lapworth, A.M. MacDonald, S. Pedley, R.G. Taylor, and J.S.T. Ward. 2018a. Real-time detection of faecally contaminated drinking water with tryptophan-like fluorescence: Defining threshold values. *Science of the Total Environment* 622–623: 1250–1257.
- Sorensen, J.P.R., A. Vivanco, M.J. Ascott, D.C. Goody, D.S. Read, C.M. Rushworth, J. Bucknall, K. Herbert, I. Karapanos, L.P. Gumm, and R.G. Taylor. 2018b. Online fluorescence spectroscopy for the real-time evaluation of the microbial quality of drinking water. *Water Research* 137: 301–309.
- Sorensen, J.P.R., A. Sadhu, G. Sampath, S. Sugden, S. Dutta Gupta, D.J. Lapworth, B.P. Marchant, and S. Pedley. 2016. Are sanitarian interventions a threat to drinking water supplies in rural India? An application of tryptophan-like fluorescence. *Water Research* 88: 923–932.
- Sorensen, J.P.R., D.J. Lapworth, B.P. Marchant, D.C.W. Nkhwa, S. Pedley, M.E. Stuart, R.A. Bell, M. Chirwa, J. Kabika, M. Liemisa, and M. Chibesa. 2015. In-situ tryptophan-like fluorescence: A real time indicator of faecal contamination in drinking water supplies. *Water Research* 81: 38–46.
- Sun, F., W. Zong, R. Liu, J. Chai, and Y. Liu. 2010. Micro-environmental influences on the fluorescence of tryptophan. *Spectrochimica Acta Part A: Molecular and Biomolecular Spectroscopy* 76: 142–145.
- Toride, N., F. Leij, M. van Genuchten. 1999. The CXTFIT code for estimating transport parameters from laboratory or field tracer experiments, research report no. 137, 119 p. US Salinity Laboratory, Agricultural Research Service, USDA, Riverside, California.
- Toride, N., F.J. Leij, and M.T. Van Genuchten. 1993. A comprehensive set of analytical solutions for nonequilibrium solute transport with first-order decay and zero-order production. *Water Resources Research* 29: 2167–2182.
- Wagner, M. 2014. *DOC-Analytik mittels 2D-Fluoreszenz-Spektroskopie (Kurztitel), Charakterisierung und Quantifizierung natürlicher organischer Wasserinhaltsstoffe mittels Fluoreszenzspektroskopie*, Dissertation, 64. DVGW-Technologiezentrum Wasser.